Case Study

LiDAR-RGB Data Fusion for Four-Dimensional UAV-Based Monitoring of Reinforced Concrete Bridge Construction: Case Study of the Fern Hollow Bridge Reconstruction

Yingbo Zhu, S.M.ASCE[1]; John C. Brigham, M.ASCE[2]; and Alessandro Fascetti, A.M.ASCE[3]

Abstract: The complexity of large-scale bridge construction necessitates continuous monitoring to perform quality assurance and control, both of which have a great influence on structural performance and durability. Conventional approaches to monitoring bridge construction heavily rely on human inspection and expert judgment performed on-site by trained technicians. However, these often lack the required spatial and/or temporal resolution in the obtainable data, and are inefficient and potentially dangerous for the operators. In this context, the development of automated systems and advanced sensing solutions brings the opportunity to enhance accuracy and efficiency, minimize human error, and mitigate safety risks. Laser scanning technology, known for its precision in target representations, combined with uncrewed aerial vehicles (UAVs) serving as multifunctional sensor platforms, are a promising means for safe and efficient monitoring of bridge construction. This manuscript presents an experimental case study focused on the application of UAV-based LiDAR-RGB data fusion for bridge reconstructions, to assess their effectiveness in monitoring bridge construction. Four-dimensional models of the bridge were constructed based on data collected via LiDAR and photogrammetry. The models generated with the two approaches then were compared formally with the target design values to ascertain their accuracy. The results demonstrate that construction monitoring strategies that only rely on photogrammetric information can provide results with insufficient accuracy, particularly in terms of the integrity of the three-dimensional (3D) reconstructions and the accuracy of the geometry and slope of the bridge superstructure. In contrast, LiDAR-RGB data fusion can provide precise and comprehensive spatial information on bridge construction, such as global and local geometry of the bridge and information on the positioning of different structural elements in the deck, which can significantly benefit construction management and construction quality assessment and control. **DOI: 10.1061/JCEMD4.COENG-15411.**

Author keywords: Uncrewed aerial vehicles (UAVs); LiDAR; Photogrammetry; Bridge construction.

Introduction

As a result of the advances in materials science, reality capture, computer vision, robotics, and artificial intelligence, the construction of civil infrastructure has witnessed significant changes over the last 2 decades (Parsamehr et al. 2023). Moreover, the need for sustainable materials and designs, which directly involve the use of digital design strategies, resulted in a steady increase in prefabrication. The quality of construction plays a central role in the performance of a structure over its lifespan. Factors such as incorrect placement of reinforcements and discrepancies in structure dimensions can lead to improper construction, which may result in premature structural failure. Consequently, there is a critical need for continuous inspection and monitoring throughout the construction process to ensure the safety and quality of the structures.

UAV-Based Monitoring and Inspection

One of the most promising monitoring and inspection strategies is the use of uncrewed aerial vehicles (UAVs). Their relative ease of use and potential for navigating complex environments, enabling inspection of hard-to-reach areas, make UAVs well-suited for tackling construction quality assurance and quality control (QA/QC) tasks (Uddin 2008). In the civil engineering field, the majority of research on UAV-based equipment focuses on the integration of imaging and photogrammetry systems onto UAVs in order to assist inspectors in acquiring visual data and digitalizing the inspection process. Dorafshan and Maguire (2018) and Zhong et al. (2018) explored the potential of employing UAVs equipped with cameras in a hovering state to detect concrete cracks. Seo et al. (2018) proved that UAVs integrated with camera sensors are capable of identifying damage in bridges, such as spalling, corrosion, and cracking. Benzon et al. (2022) introduced an approach to create structural digital twins based on images collected using drones. UAVs equipped with infrared (IR) thermography sensors also have garnered considerable attention. Ellenberg et al. (2016) and Omar and Nehdi (2017) integrated infrared cameras into UAVs to rapidly detect and estimate delamination in bridge decks. Mac et al. (2019) examined the effectiveness of a handheld infrared thermography camera and a UAV equipped with an IR camera in detecting

[1]Graduate Student Researcher, Dept. of Civil and Environmental Engineering, Univ. of Pittsburgh, Pittsburgh, PA 15261 (corresponding author). ORCID: https://orcid.org/0000-0002-8938-6506. Email: yiz189@pitt.edu

[2]Associate Professor, Dept. of Civil and Environmental Engineering, Univ. of Pittsburgh, Pittsburgh, PA 15261. Email: brigham@pitt.edu

[3]Assistant Professor, Dept. of Civil and Environmental Engineering, Univ. of Pittsburgh, Pittsburgh, PA 15261. ORCID: https://orcid.org/0000-0003-4289-5909. Email: fascetti@pitt.edu

Note. This manuscript was submitted on April 1, 2024; approved on July 15, 2024; published online on October 26, 2024. Discussion period open until March 26, 2025; separate discussions must be submitted for individual papers. This paper is part of the ***Journal of Construction Engineering and Management***, © ASCE, ISSN 0733-9364.

concrete delamination up to a depth of 40 mm in concrete. Moreover, alternative sensors such as laser Doppler vibrometers (Garg et al. 2019) and reflector prisms (Jimenez-Cano et al. 2019), have been mounted on UAVs to estimate bridge deflections.

LiDAR Technology in Civil Engineering

A technology that can facilitate the inspection and monitoring of infrastructures is light detection and ranging, commonly known as LiDAR. LiDAR is a noncontact method that can evaluate the distance from a target by sending a detection signal (i.e., a laser beam) and measuring the time from transmission to reception (González-Jorge et al. 2016; You et al. 2023). Compared with conventional measuring approaches, LiDAR can improve efficiency and spatial resolution, and provide safer operations. Based on their movement patterns, LiDAR scanning systems can be subdivided into two categories: terrestrial laser scanning (TLS), and airborne laser scanning (ALS). TLS systems, which are tripod-based, require trained personnel to position the scanning device on a tripod at predetermined locations to capture three-dimensional (3D) models of target objects. The capability of TLS to generate dense point clouds with high accuracy and resolution, combined with the relatively low cost and ease of use, have made them instrumental in monitoring and assessing conditions in civil infrastructure (Cha et al. 2019; Xu et al. 2022). For example, several studies (Qureshi et al. 2024; Wang et al. 2017; Yuan et al. 2021) adopted TLS-collected point clouds to automatically evaluate the quality, spacing, and positions of rebar installment. Other researchers (Puri and Turkan 2020) employed LiDAR systems to monitor the bridge construction process, and then compared the percentage of completion for the as-built bridge components with the as-planned value to better track the completion of the bridge components.

In contrast, ALS systems, which often are integrated with UAVs, are a mobile and versatile approach. UAV-mounted LiDAR systems offer the advantage of accessing challenging or hazardous locations, and also provide the flexibility of remote or autonomous control, enabling scanning and monitoring of large-scale targets. Consequently, ALS has gained popularity in mapping and surveying tasks of so-called macrotargets (e.g., forests, rivers, and large-scale urban areas) for the acquisition and analysis of global features (Ariyachandra and Brilakis 2020; Resop et al. 2019; Shirowzhan et al. 2021; Trepekli et al. 2022; Wallace et al. 2012). In contrast to macrotargets, civil engineering applications often aim at mapping and monitoring so-called microtargets (e.g., bridge elements and building features), requiring a much higher degree of spatial accuracy and resolution. Achieving accuracy at the centimeter level when monitoring a microtarget using UAV-based LiDAR systems poses several scientific and technical challenges, which is the object of ongoing studies in many research groups. As a result, available research on monitoring microtargets in civil engineering still is limited. Karan et al. (2014) adopted UAV-mounted LiDAR to construct digital terrain models of construction sites, whereas Cheng et al. (2015) adopted an airborne LiDAR system to evaluate the dimensions of bridge structures. He et al. (2016) developed a 3D shape descriptor to analyze post-event airborne LiDAR point clouds in order to detect damage caused by earthquakes, which proved to be accurate in detecting surface and structural damage. Fascetti and Oskay (2019) developed a photogrammetry- and LiDAR-based monitoring system to reconstruct the local geometry of river levees in the context of erosion analyses. Yuan et al. (2023) proposed an algorithm to automatically evaluate the reinforcement spacing at a bridge construction site using a mobile LiDAR system.

LiDAR-RBG Data Fusion in Civil Engineering

Fusion of LiDAR-RBG data is a popular approach for generating high-quality visual representations of objects by combining the 3D LiDAR point cloud data with the two-dimensional (2D) imagery. This approach can significantly improve the interpretability of the collected data, as well as the accuracy in recognizing local and global geometries. Data fusion is used widely in medical image analysis, computer vision, and earth observation, and is being applied to civil engineering to better complement automatic monitoring and inspection techniques (Sohn and Dowman 2007). Trzeciak and Brilakis (2023) proposed a pipeline to improve the readability and quality of the LiDAR point cloud by fusing it with 2D imagery. An et al. (2022) proposed an algorithm to fuse the LiDAR and RGB information to extract the geometric information of structural assemblies. Yan et al. (2021) developed a LiDAR-RGB data fusion approach to detect cracking in concrete columns.

Available Methodologies for Bridge Construction Monitoring

Traditionally, bridge engineers have relied on visual inspections to monitor and assess construction quality. This approach requires inspectors to hold field equipment and paper-based documentation to record the structural conditions that they visually infer. This procedure may take as much as several days to complete in the case of large-scale bridge structures, and the inspection is being dependent on the expertise of the operators. Moreover, bridge construction sites generally are difficult to navigate and potentially dangerous for inspectors (e.g., operators often are required to use scaffolding or special cars equipped with robot arms to inspect the superstructure of a bridge).

In recent years, various technologies have been introduced to enhance conventional monitoring and inspection approaches in order to reduce human error and personnel safety risks while improving efficiency. Table 1 reports a synthetic description of available methodologies. Starting from the early 1990s, Global Positioning System (GPS)-based wireless technologies have been used to monitor bridge construction. Okamoto et al. (1997) employed GPS to locate the caisson during bridge construction, ensuring accurate placement in water, and Navon and Shpatnitsky (2005) employed GPS technology to estimate the earthmoving performance by tracking equipment positions. Although GPS facilitates real-time tracking of equipment and components during construction, capabilities are limited to local positional observations that generally are spatially sparse, as a result of the necessity of physically attaching receivers to the physical entities to monitor. Additionally, GPS measurements generally are less accurate in the vertical direction (i.e., the direction of gravity), posing challenges in applications requiring low vertical tolerances, and also are dependent on satellite availability, weather conditions, and environmental factors. In recent years, advancements in machine learning and artificial intelligence have led to computer vision–based techniques being proposed for bridge construction monitoring tasks (Bai et al. 2012; Ju et al. 2012; Spencer et al. 2019; Zhang et al. 2024). Although these techniques can provide global information on construction schedules, the accuracy of the measurements still is limited as a result of challenges in camera resolution, potential lens distortion, motion blurring in the presence of highly dynamic environments, limited depth information, and varying environmental conditions. Therefore, LiDAR systems have gained significant popularity in bridge structural monitoring due to their higher accuracy. Laser-based measurements can provide accurate 3D reconstructions of bridge structures, and the positions of components can be determined precisely by analyzing

the obtained point clouds (Jiang et al. 2022). However, a limitation of LiDAR technology is its inability to capture textural information, which can be essential for comprehensive monitoring and 3D visualization. Both the computer vision–based and LiDAR-based methodologies have advantages and limitations. Integrating these two methodologies in a UAV-based platform has the potential to retrieve accurate geometric information while also providing rich textural details of bridge structures during the construction process in the context of QA/QC.

Research Significance and Objective

As described in the previous section, the available literature highlights the capabilities of various sensors to augment traditional inspection methodologies for structural assessment of civil infrastructure, addressing issues such as concrete cracking, steel corrosion, and delamination. However, comparatively less attention has been devoted to monitoring construction quality for large-scale bridge systems, which requires mapping of environments that are inherently complex to navigate. Automated inspection and monitoring have the potential to offer greater insights for effective construction QA/QC and provide efficient methodologies to enable maintenance optimization (Wang and Yin 2022). However, more research is needed in order to define best practices in data acquisition and processing, data analysis, and feature extraction in reconstructed scenes. Therefore, this manuscript reports a case study focused on monitoring the construction of a prestressed RC bridge using UAV-based LiDAR-RGB data fusion, in order to analyze the potential to facilitate construction QA/QC of structures. Specifically, the reconstruction of the Fern Hollow Bridge in Pittsburgh, Pennsylvania is presented.

To the best of the authors' knowledge, this is the first study reporting four-dimensional information on bridge construction by means of UAV-based operations. This experimental campaign not only provides a comprehensive data set of LiDAR data and imagery on a significant infrastructure component that recently was rebuilt after a collapse, but also serves as a valuable example of the application of the LiDAR-RGB data on construction QA/QC, in the form of grade and slope evaluation and geometrical tolerance analysis. The main objectives of this study were to

1. perform the qualitative and quantitative analysis of the quality of the LiDAR-RGB and photogrammetry point clouds collated by the UAV-based system;
2. analyze global and local geometrical features of the bridge over time, such as grade and component sizes, using the obtained LiDAR-RGB and photogrammetry point clouds to validate the effectiveness and feasibility of the UAV-based monitoring system for bridge construction; and
3. analyze influencing factors, such as flight speed and environmental conditions, on the quality of the collected data.

The Fern Hollow Bridge Reconstruction

Background

The object of the presented case study is the Fern Hollow Bridge reconstruction, located in Pittsburgh, Pennsylvania. The old Fern Hollow Bridge collapsed on January 28, 2022 [Fig. 1(a)], primarily due to the deterioration of the weathered steel on the north side of the bridge (NTSB 2023). Due to the importance of the bridge to the local community in connecting two of Pittsburgh's neighborhoods, rapid demolition and reconstitution of the bridge were required.

The Fern Hollow bridge replacement was designed as a three-span continuous prestressed RC bridge with integral abutments. A total of 21 prefabricated I-beams with depth of 2.4 m and a length of 46.8 m were used to span the design length of 140.2 m [Fig. 1(e)]. The cross section of the bridge is reported in Fig. 1(d); it has a total deck width of 19.5 m (out-to-out), including four 3.05-m-wide traffic lanes, two 0.6-m-wide shoulders, 1.5- and 3.2-m sidewalks, plus barriers. The thickness of the deck was designed as 0.229 m. The substructure comprises four circular column piers with a diameter of 2.59 m. A view of the completed replacement bridge is shown in Fig. 1(c).

Table 1. Current methodologies for bridge construction monitoring

Method	Advantages	Disadvantages	Remarks
Visual inspection	Easy implementation	Time-consuming Labor-intensive Relies on expertise of inspectors Challenges in navigating complex environments	Applied to all bridges
GPS-based wireless method	Real-time position High accuracy Safety improvement	Local observations Does not allow for monitoring of surrounding environment Potential signal obstruction Sensitive to environmental conditions Maintenance and calibration	Aims to measure position of bridge components
Image- or video-based method	Timely monitoring Rich textural information Safety improvement	Accuracy is highly dependent on environmental conditions Lack of spatial accuracy or depth information	Use of computer vision technologies to extract meaningful information
LiDAR-based method	High accuracy Less affected by environmental conditions Can be integrated into uncrewed solutions	High initial costs Lack textural information	Direct measurement of target geometry

J. Constr. Eng. Manage., 2025, 151(1): 05024016

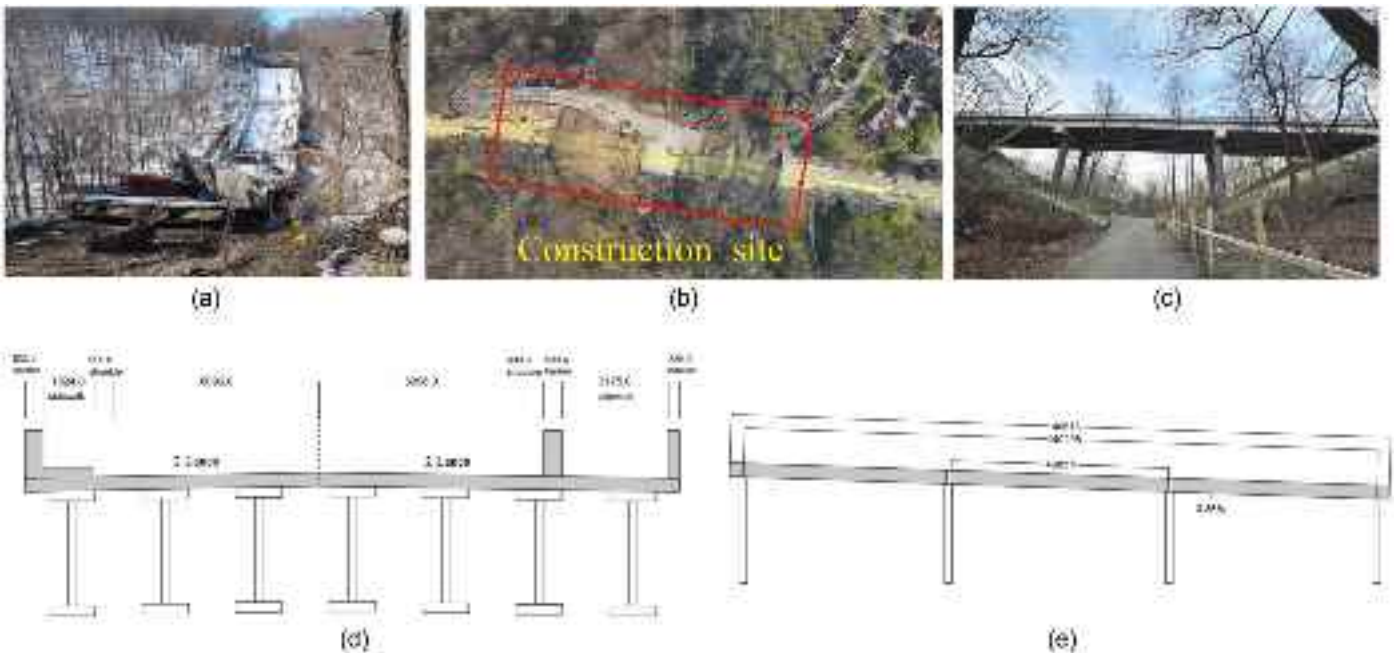

Fig. 1. Fern Hollow Bridge: (a) collapse of the old bridge (reprinted from NTSB 2023); (b) construction site area (Imagery ©2024 Airbus, Maxar Technologies, Map data ©2024); (c) completed bridge replacement (image by Yingbo Zhu); (d) design cross section of the bridge replacement (data from Pennsylvania DOT 2022); and (e) longitudinal profile of the bridge replacement. All units are in millimeters.

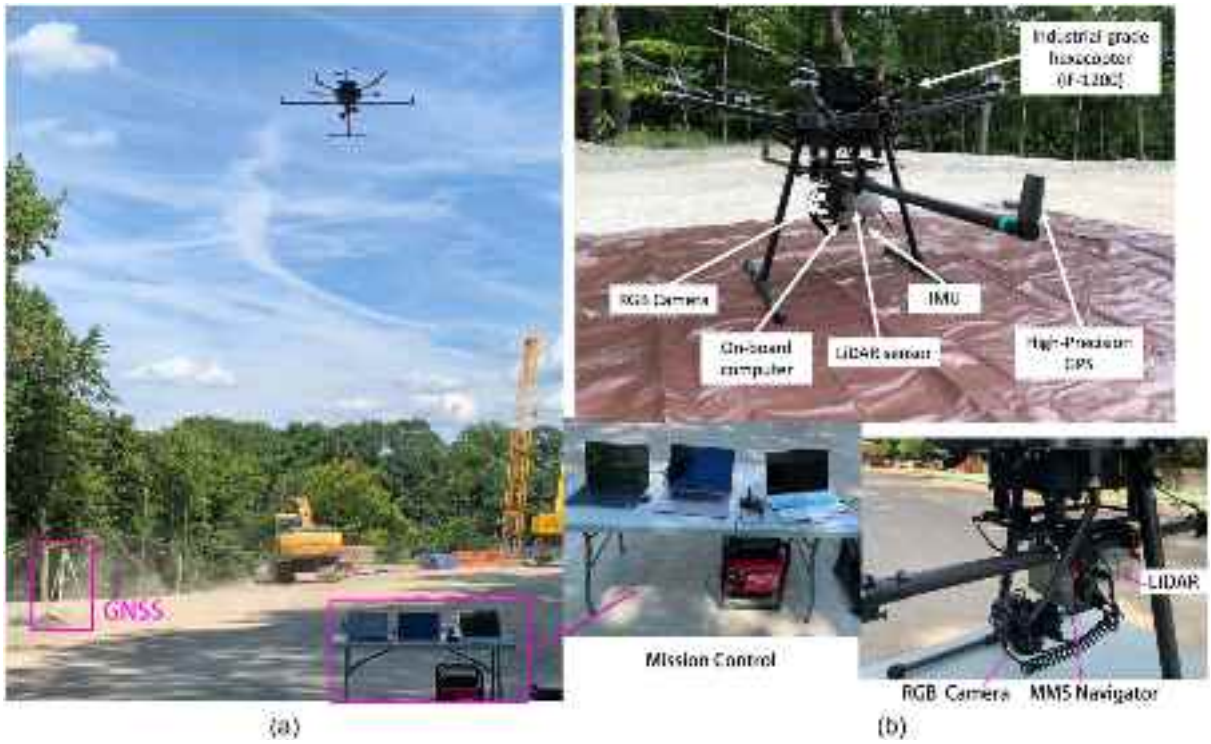

Fig. 2. LiDAR/photogrammetry data acquisition system: (a) overall view of the flight operations; and (b) details of UAV, mission control, and onboard instrumentation. (Images by authors.)

Experimental Setup

The UAV used in this study was an IF1200 hexacopter (Inspired Flight, San Luis Obispo, California) (Fig. 2), which is a heavy-lift, fixed-wing system that can integrate multiple surveying and mapping systems. The maximum payload of the drone is 8 kg, with a corresponding maximum flight time of 40 min. The employed surveying system comprises four primary components: a mobile

mapping system (MMS) Navigator (Geodetics, Solana Beach, California), LiDAR scanner, RGB camera, and GPS antennas. The MMS Navigator is a real-time dual GPS-assisted inertial navigation system offering both real-time kinematics (RTK) and postprocessed kinematics (PPK). The Navigator consists of a high-precision inertial measurement unit (IMU), a GPS receiver, an onboard computer equipped with a dual-core processor, and a data recorder. The LiDAR scanner used in this study was a Velodyne (San Jose, California) HDL-32E, with 360° vertical and 41° horizontal fields of view. The sensor can generate as many as 0.7×10^6 points/s with centimeter-level accuracy in a single return mode at a range of 100 m. In addition, the measurement platform integrates an RGB Sony α6100 (Tokyo) camera equipped with a 20-mm lens to capture nadir imagery during operations. The use of both LiDAR and photogrammetric sensors accomplished a twofold goal of this study: (1) the RGB images can be processed separately using traditional photogrammetry to create a complementary set of point clouds to perform a formal comparison of RGB- and LiDAR-based monitoring systems, and (2) orthomosaic images are used to perform data fusion and project color information on the LiDAR point clouds. One of the main advantages of the MMS Navigator is that it allows direct georeferencing of the acquired data. In all the missions described herein, PPK was used to obtain detailed information on the flight path and georeference the LiDAR and RGB data, by employing a GNSS antenna as ground control [Fig. 2(a)].

Flight Plan and Mission Control

The flight path design can significantly impact the data quality of the UAV-based LiDAR and RGB systems (Battulwar et al. 2020). The overall objective in designing efficient flight paths is to generate a dense point cloud with enough resolution and target representation while minimizing flight time and the required number of strips (i.e., the longitudinal passes along the axis of the bridge). Fig. 3 reports the typical flight path used in all the UAV missions reported herein; there were a total of four longitudinal strips. The space between two adjacent strips was selected to be 15 m to ensure sufficient side overlap.

QGroundControl (QGC) software version 4.0.11 was used to generate the flight path data to be uploaded on the UAV's internal controller. The same location at the west end of the bridge was used for both take-off and landing. The other side of the bridge (the east side) lies in proximity to a residential area, limiting flight reach for safety reasons. Detailed considerations were required to assess the optimal target distance (i.e., flight elevation). Due to the complex environmental conditions and the presence of construction equipment such as cranes, the altitude was set to 50.29 m to ensure sufficient vertical clearance from obstacles while at the same time allowing for sufficient resolution in the obtained data. Flight speeds ranging from 8.05 to 11.26 km/h were used, depending on the wind conditions at the site, which also allowed exploring the impact of flight speed on the quality of the obtained point clouds.

Although the LiDAR scanner is relatively unaffected by the weather conditions, the quality of the RGB imagery is highly dependent on lighting conditions. Therefore, to the best of the authors' abilities, flight missions were scheduled in the early afternoon on sunny days to optimize photo quality. The research team coordinated with the construction company to perform scans at times when construction was halted and no workers were on site (i.e., on the weekends). A total of five missions were conducted to comprehensively monitor and assess the bridge construction process during the main construction stages. Each mission corresponded to a major construction phase: Mission 1 was conducted after the installation of the I-beams, Missions 2–4 were executed during the construction of the bridge deck, and Mission 5 was carried out after the bridge deck was completed.

LiDAR-RGB Postprocessing and Data Fusion

Fig. 4 reports the workflow for the postprocessing of the obtained data. As mentioned, the system used provides both RTK and PPK functionalities. To achieve high positional accuracy, PPK differential GPS processing was chosen for georeferencing both the LiDAR data and the aerial imagery. The obtained geotagged aerial images were processed using structure-from-motion photogrammetry to create a set of point clouds and orthomosaic images. Orthomosaic images are a distortion-free representation of nadir aerial photos that undergo geometric orthorectification, providing a single georeferenced top-down view of the target.

The raw data collected by the LiDAR scanner were processed in the proprietary LiDARTool version 1.0 software to obtain georeferenced LiDAR point clouds for each of the four flight strips in each mission. For the postprocessing of LiDAR point clouds, the statistical outlier removal (SOR) method (Rusu et al. 2008) was used to identify outliers in the LiDAR raw data. Then the point cloud strips were aligned preliminarily using the iterative closest point (ICP) method (Chetverikov et al. 2002), which can improve the efficiency of the operation, and a subsequent fine alignment was performed manually to ensure maximum accuracy. Finally, RGB information from the orthomosaic images was projected vertically on the LiDAR point cloud to finalize the data fusion between the

Fig. 3. Typical flight path used for data acquisition. (Imagery ©2024 Airbus, Maxar Technologies, Map data ©2024).

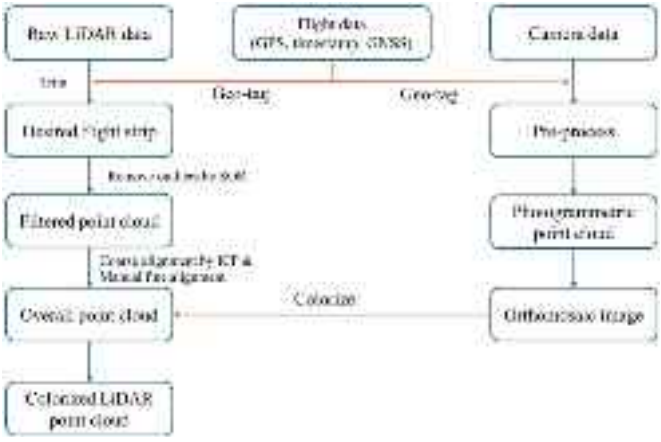

Fig. 4. Workflow employed for data processing.

two data sets. To enable accurate colorization of the LiDAR point clouds, all orthomosaic images were exported using a pixel resolution of 2 cm. Final manual inspection and fine-tuning (if needed) were performed to ensure satisfactory alignment of the two sets.

The postprocessing of the collected LiDAR data and aerial imagery is a time-demanding task requiring specific expertise from the user, particularly in addressing the alignment challenges between different strips, the alignment between different point clouds and the orthomosaic image (to perform data fusion), and the extraction of features of interest and corresponding data. These alignment challenges inevitably affect the accuracy of LiDAR-RGB data fusion, as analyzed quantitatively subsequently.

Four-Dimensional Modeling of Bridge Construction

Orthomosaic Images

Because the distortions resulting from the camera lens and topography are eliminated, the orthomosaic images are true to geography, and can be used in construction QA/QC operations by direct comparison of the geotagged images to assess compliance to design and as-built information. The orthomosaic images obtained from the performed missions are reported in Fig. 5. From the top view, the images provide a high-resolution depiction of the state of the system, revealing details such as the positioning of construction equipment, reinforcements, and wooden curing formwork.

The first orthomosaic image shows the installed precast I-beams and the wooden forms on both sides of the edge beams. Subsequently, on September 10, 2022, longitudinal and transverse reinforcements were set up on the west side span, and the ongoing installation of reinforcements on the mid-span bridge deck was carried out in the following 2 weeks (Mission 3). Between September 24 and October 8, the reinforcement of the east side span was finalized, and finally the concrete deck was cast in place. The final flight mission shows the construction process of the concrete deck near completion. The orthomosaic images provide a comprehensive assessment of the progression of the bridge construction, including the location of equipment, the status of operating tasks, and structural details such as the layout of steel rebars, serving as a valuable resource for construction management. Some of the bridge parameters, such as length and width, and the spacing between steel rebars can be measured precisely. However, due to the nature of vertical projection, many geometrical features, such as depth or vertical distances between elements, cannot be retrieved from the orthomosaic imagery.

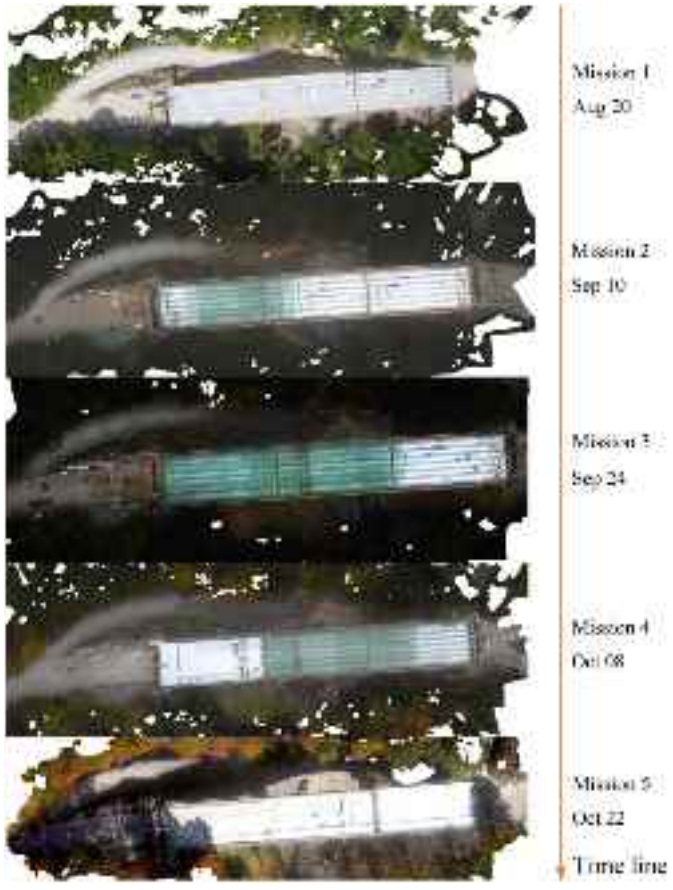

Fig. 5. Orthomosaic images at different construction phases.

LiDAR and Photogrammetry Point Clouds

The LiDAR point clouds were colorized using data fusion with the orthomosaic images, as described previously, and the resulting data set is shown in Fig. 6. Fig. 6(a) shows the final alignments of the raw LiDAR point clouds. The alignment of point clouds shows that the overlap of the bridge deck among the three flight strips was close to 100%, allowing for high accuracy in the alignment process. Fig. 6(b) presents the overall visualization of the fused point clouds, which provide a much higher degree of explainability of the

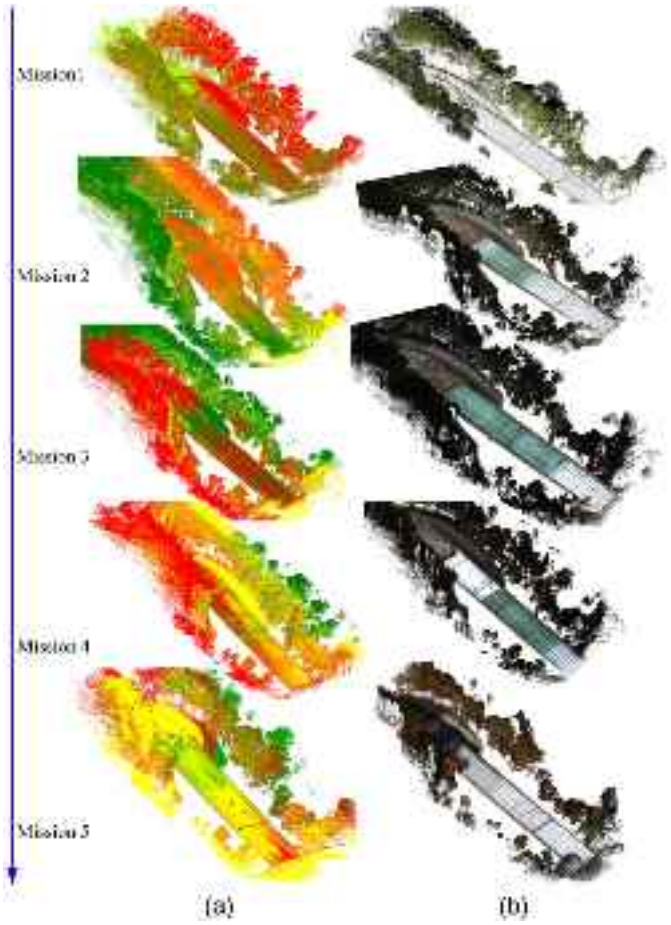

Fig. 6. Obtained LiDAR point clouds: (a) aligned LiDAR point clouds; and (b) finalized LiDAR-RGB point clouds.

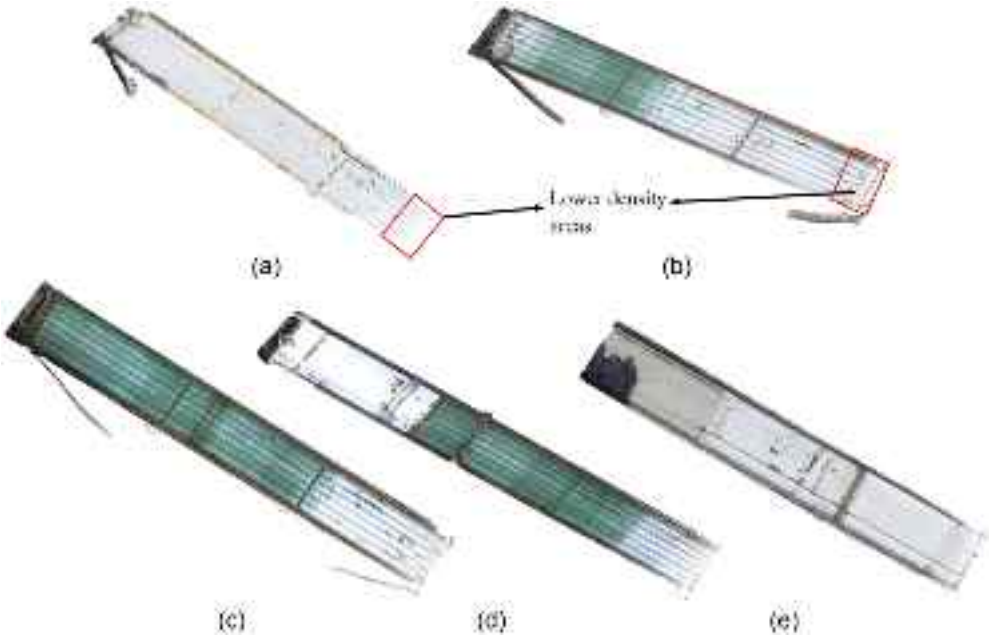

Fig. 7. Detailed view of the Fern Hollow reconstruction bridge deck: (a) Mission 1; (b) Mission 2; (c) Mission 3; (d) Mission 4; and (e) Mission 5.

3D scenes than the raw point clouds, both to human operators and for computer vision–based approaches (Luo et al. 2016).

In addition, Fig. 7 reports a detailed view of the bridge deck, obtained from the segmentation of the colorized point clouds. The reconstruction of the bridge deck from the LiDAR-RGB data set provides a clear representation of several important elements. For example, the location and geometrical features of reinforcing bars, wooden forms, and equipment on the bridge deck can be retrieved. Overall, colorized point clouds of the bridge deck can enable construction managers to perform construction QA/QC effectively by facilitating both direct inspection and measurement of areas of interest. For example, the coordinates or locations of I-beams, equipment, and molds; the width and length of the bridge deck; and even the layout of reinforcements can be extracted directly.

For comparison purposes, Fig. 8 reports the point clouds generated using traditional photogrammetry by employing the geotagged nadir imagery data set. As expected, the point clouds generated from photogrammetric techniques are less accurate than those obtained from the LiDAR data. For example, the I-beams in Missions 2–3 are only partially reconstructed as a result of occlusion in the images, and the point clouds generated by photogrammetry have a higher level of noise and distortions.

Quality Assessment of Point Clouds

Qualitative Analysis

Figs. 6–8 report the point clouds obtained by LiDAR-RGB data fusion and photogrammetry. Visual comparison indicates that the LiDAR point clouds can provide superior 3D models of the construction site compared with photogrammetric point clouds. Specifically, photogrammetry failed to reconstruct the full geometry of the RC I-beams (Missions 3–4), as a result of the lower contrast in the aerial images. Insufficient contrast in the data can result in imperfect alignment between neighboring images, particularly for objects with a relative lack of geometrical and/or color features such as the I-beams, ultimately resulting in inconsistent point clouds. A similar phenomenon occurred on the west side span bridge deck in Mission 5, where the concrete deck was partially obscured by surrounding vegetation. The lack of distinct features in the shadowed area led to inaccurate point cloud reconstructions. In addition, some regions of the bridge deck that were obscured by the on-site equipment also posed challenges in the photogrammetric reconstruction [Fig. 8(c)]. In contrast, LiDAR data are less affected by environmental conditions such as weather and lighting, ultimately resulting in denser, more-accurate point cloud representations.

Moreover, Fig. 9 shows the side views obtained from the point clouds generated by the two approaches. The LiDAR point clouds present a more detailed and accurate representation of the bridge, particularly in terms of capturing the bridge grade, which is highly consistent throughout each mission. In contrast, the photogrammetric point clouds have a higher level of noise and provide a highly variable, and thus inaccurate, description of the grade of the bridge.

Quantitative Analysis

The spatial density of the obtained point clouds can be used as an indicator of the quality and resolution of the reconstructed scenes. Because the bridge superstructure was the main focus of the present work, the density of the bridge deck point cloud was analyzed quantitatively. Fig. 10 reports the point cloud surface density obtained from a single strip in each mission. The surface density was calculated as the total number of points in a circular region with a radius 0.1 m divided by its area. In each mission, the surface density of the west side span was much higher than that of the east side, approximately 700–1,100 versus 100–300 points/m^2. This disparity can be attributed to the generated flight paths, as mentioned previously. Fig. 11 provides detailed statistics of the surface density obtained from each mission, and indicates a normal distribution. The mean values for Missions 1–3 were approximately 675, 635, and 540 points/m^2, respectively, whereas the mean values observed from Missions 4 and 5 were approximately 790 and 795 point/m^2, respectively. As expected, the point density increased with decreasing flight speed. However, despite variations among the five missions, all point clouds had very high resolution, with a surface density exceeding 500 points/m^2 in all cases.

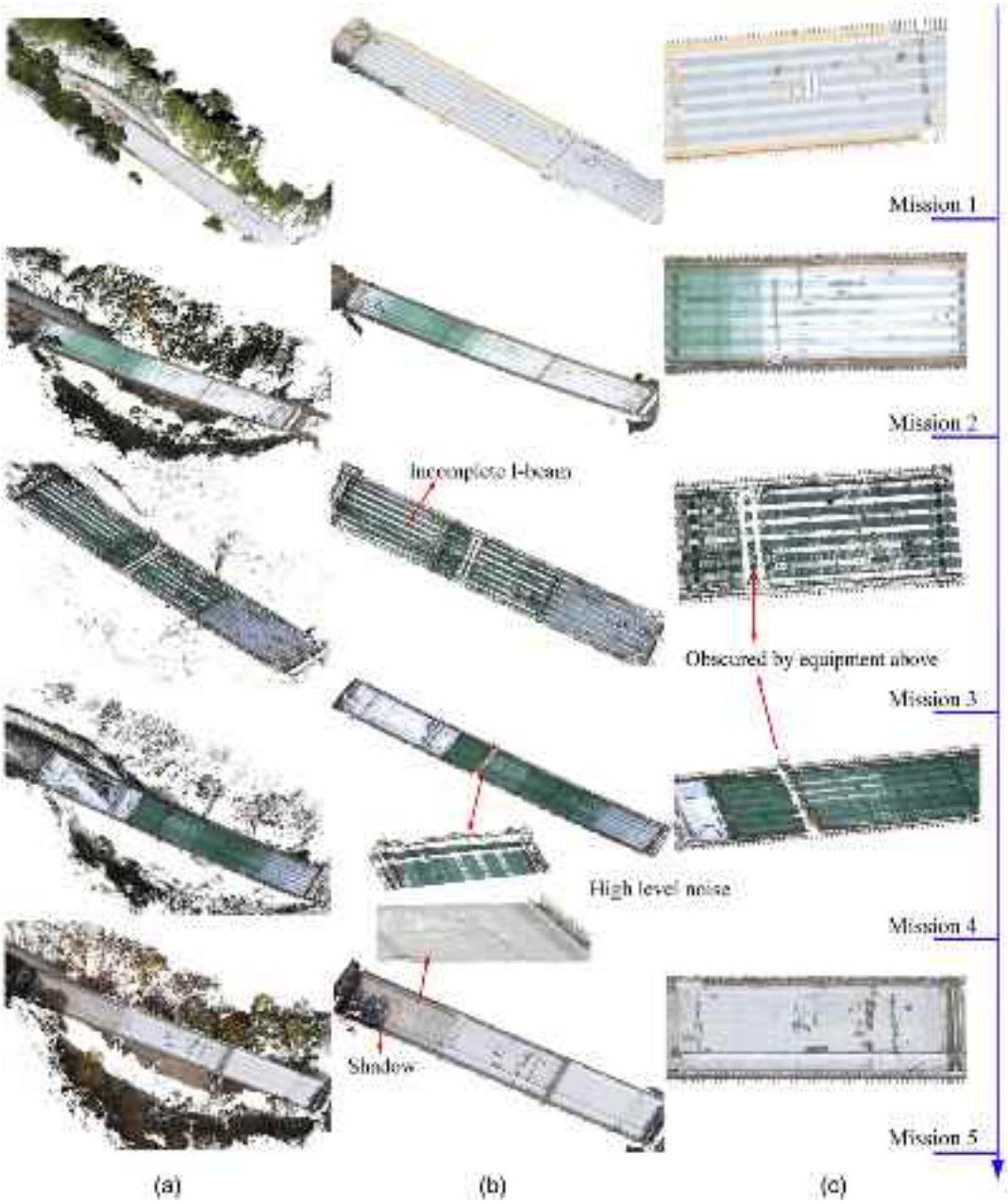

Fig. 8. Photogrammetric point clouds: (a) overall view of the construction site; (b) bridge deck; and (c) details of the midspan of the bridge deck.

Facilitating Construction QA/QC Using LiDAR-RGB Data Fusion

One major goal of this work is to serve as a case study for the application of LiDAR-RGB data fusion in facilitating bridge construction QA/QC. For example, the obtained data sets can be used to characterize the geometrical features of various components within the bridge, such as beams, concrete formwork, and longitudinal and transverse reinforcements by direct measurements, which then can be compared with their design values. Furthermore, the data sets also have the capability to monitor structural displacements during construction by comparing subsequent phases, which potentially can provide critical information to accurately quantify the as-built state of the structure. To underscore their value and validate their accuracy, this section quantitatively compares information obtained from both the LiDAR-RGB and photogrammetric point clouds.

Monitoring the Elevation of the Bridge Superstructure

To track the elevation changes precisely across missions, an area of interest (AOI) with size 0.2×0.2 m^2 was chosen at the centerline of the bridge midspan (Fig. 12). Within the top surface of the AOI, seven points were chosen randomly from each mission, and their average elevation was evaluated. The midspan construction activity between Missions 1 and 3 primarily involved reinforcement installation, resulting in an initial elevation increase during this construction period (Fig. 12). Between Missions 3 and 4, no construction operations occurred in the inspected portion of the bridge until the surface elevation increased due to pouring of the deck. The total change in surface elevation of the superstructure evaluated from the point cloud was 241 mm, which is in good agreement with the design bridge deck thickness of 229 mm. The slight deviation can be attributed to the presence of a curing tarp on the concrete deck [Fig. 7(e), Mission 5], which added to the estimated elevation

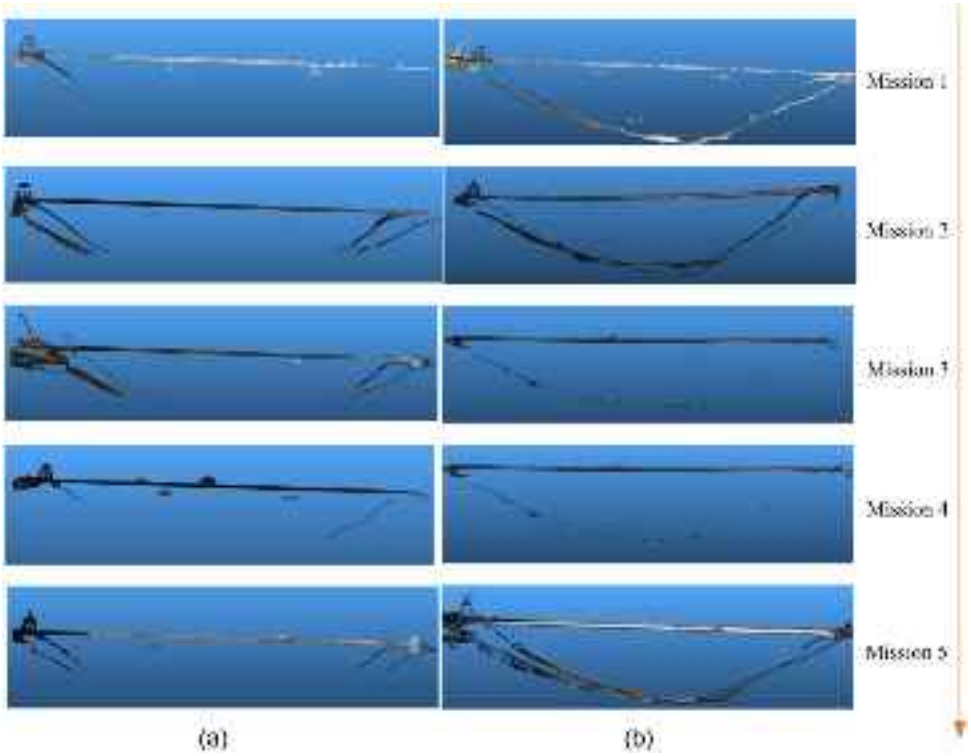

Fig. 9. Side view of the obtained point clouds: (a) LiDAR; and (b) photogrammetry.

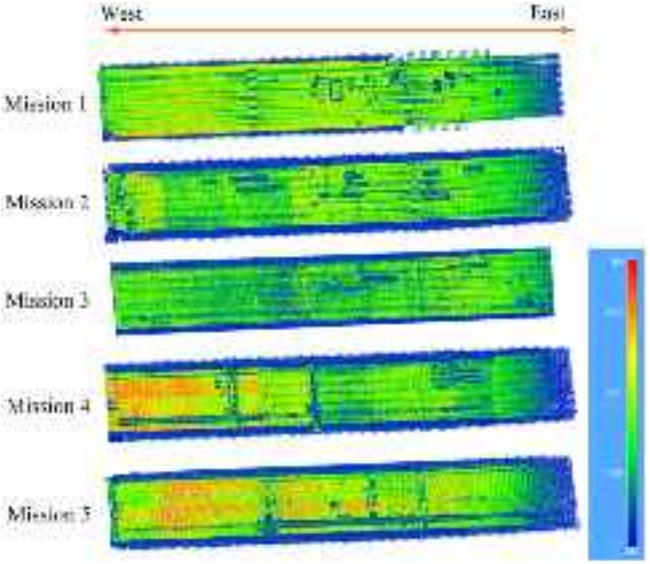

Fig. 10. Surface LiDAR point cloud density obtained from the different missions.

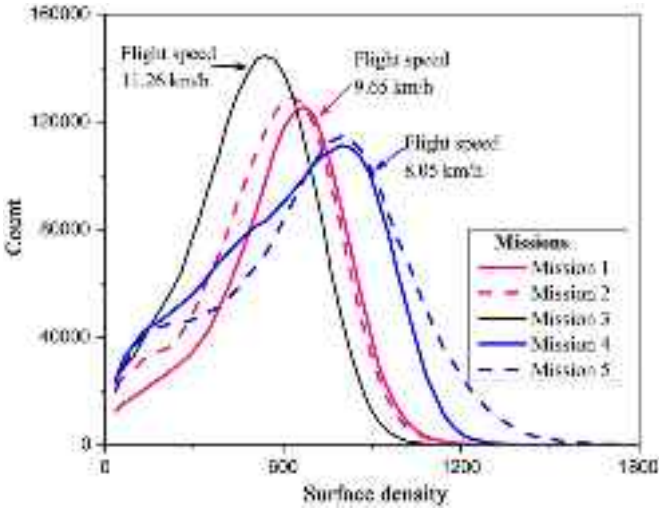

Fig. 11. Distribution of the LiDAR point cloud surface density obtained from different missions.

measurements. According to the ACI 117-10 (ACI 2010) standard, construction tolerances on exposed surface decks should be within ±19.05 mm (±3/4 in.); therefore, the obtained 12.00 mm deviation of the bridge deck is within the allowable limit.

Bridge Grade

The Fern Hollow Bridge reconstruction was designed to have a 3.36% longitudinal grade. To accurately obtain the as-built grade information and to investigate the precision of the two sets of point clouds, the grade reconstructed from each data set was obtained using the random sample consensus (RANSAC) method (Schnabel et al. 2007). RANSAC is an iterative method used to estimate model parameters by random sampling of collected data to detect the shape of representations in 3D point clouds. This method can provide not only precise results but also a robust and reproducible methodology. The bridge deck of the point cloud for each mission was fitted to a plane by RANSAC, for both the LiDAR-RGB and the photogrammetry data sets, and the grade of the bridge was obtained by analyzing the normal direction of the fitted plane

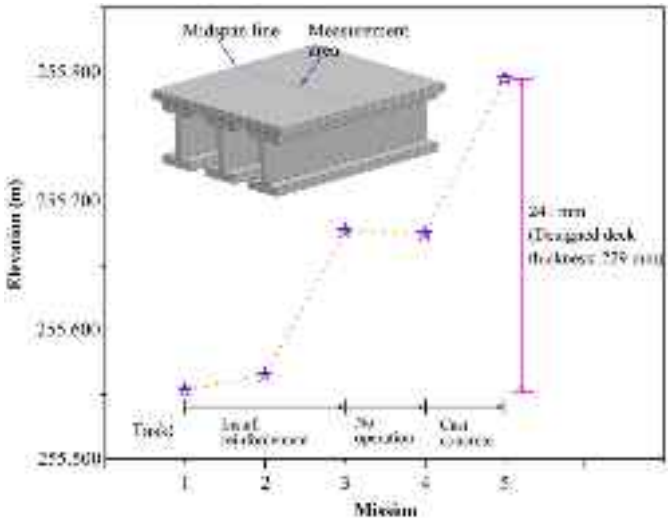

Fig. 12. Measured elevation changes in the bridge surface during construction based on the collected LiDAR-RGB data.

(Fig. 13). The grades of the bridge deck estimated by the RANSAC plane for all five missions are compared in Fig. 13(c). Values obtained from the LiDAR-RGB point clouds compared well with the design value; all were in the range 3.25%–3.5%, suggesting that the laser-based measurements can provide remarkable accuracy in the evaluation of the longitudinal grade of the bridge. For the photogrammetric point clouds, the fitted planes of the first and fifth missions achieved satisfactory agreement with the design value. However, Missions 2–4 exhibited lower values, ranging from 0% to 1.2%, as a result of severe distortion, which is evident in Fig. 9(b).

Analysis of Bridge Dimensions

For analyzing the geometry of the bridge, the following methodology is proposed: (1) 3D lines are fit using least-squares regression using a set of randomly sampled points at each end of the object to be measured (e.g., deck and I-shape beam); (2) the distance between the fitted lines is computed for each possible combination; and (3) statistical measures [i.e., mean and standard deviation (SD)] are calculated for all possible combinations.

Beam Length

To measure the length of the RC beams, a total of 15 points were selected randomly from each end of the elements at each span, and two linear curves were fitted to the selected points to represent beam ends (Fig. 14). The beam length then was estimated by measuring the distance from each point on one end to the linear fit for the opposite end; therefore, 30 measurements were obtained for each beam [Fig. 14(b)]. Fig. 14(c) and Table 2 report the measured and design values of the beam lengths for both the LiDAR-RGB and the photogrammetric reconstructions. The reconstructions obtained from the LiDAR-RGB data fusion matched the designed value with high accuracy, whereas the photogrammetric data consistently underestimated the length of the beams.

Bridge Length and Width

The total bridge length typically refers to the distance between abutment back walls; however, the abutments often are shaded by construction equipment, soil, and/or wooden molds, making it difficult to identify their locations accurately from aerial point clouds. Therefore, the bridge length was obtained herein as the distance between the west and east side ends of the I-beams [Fig. 1(e)]. The design value for the defined bridge length was 140.813 m. Similar to the protocol used to measure the length of the I-beams, 15 points were selected randomly from both ends of the bridge, and two linear curves were fitted. Then the length of the bridge was estimated by measuring the distance from each point on one end to the linear fit for the opposite end; therefore, 30 measurements were obtained. The average of all the measurements for each mission is reported in Fig. 15.

The bridge length was calculated on Missions 1–4; the presence of the curing tarp in Mission 5 rendered the localization of the endpoints impossible. The calculated length values from both sets of point clouds are presented in Table 3 and Fig. 15. For the LiDAR-RGB point clouds, the average estimated lengths were 140.727, 140.757, 140.864, and 140.970 m, respectively, agreeing well with the designed value of 140.813 m. Moreover, the obtained data had standard deviations ranging from 0.042 to 0.077 m, further highlighting the accuracy of the obtained reconstructions. In contrast, for the photogrammetric point clouds, the measured bridge lengths exhibited significant deviations from the design values across the different missions. For example, the average length calculated from Mission 1 was 140.366 m, which is lower than the design value. For the subsequent missions, the measured values for the photogrammetric point clouds were higher than the design length;

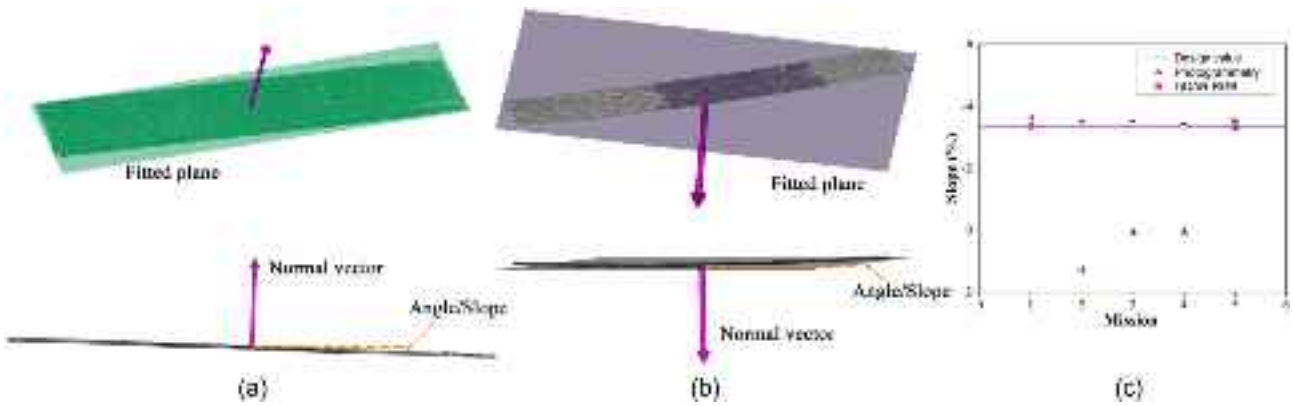

Fig. 13. Bridge grade analysis: (a) LiDAR-RGB point cloud (Mission 2); (b) photogrammetric point cloud (Mission 2); and (c) comparison of LiDAR-RGB and photogrammetric point clouds with the design value.

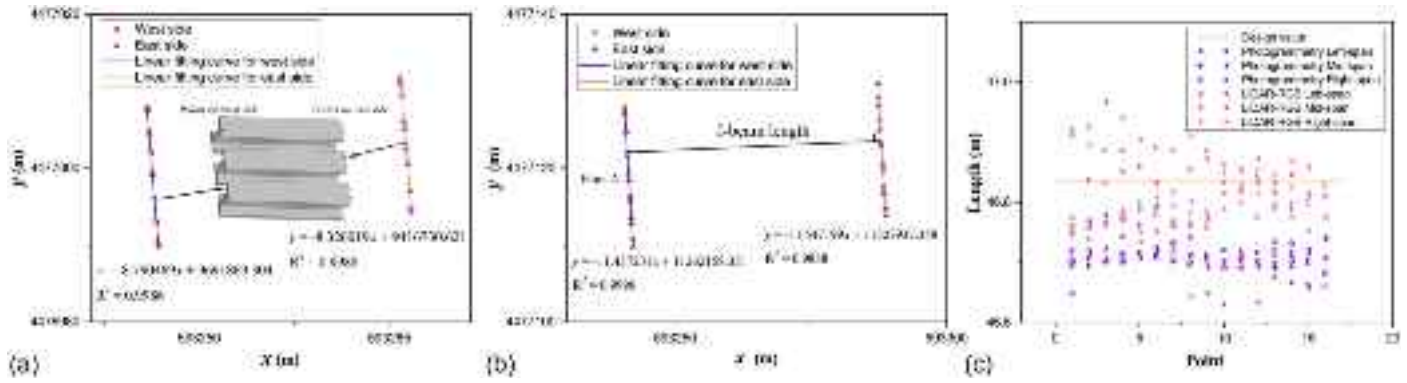

Fig. 14. Estimation of I-beams length based on Mission 1 data: (a) LiDAR-RGB; (b) photogrammetry; and (c) comparison of LiDAR-RGB and photogrammetric point clouds with the design value.

Table 2. Comparison of I-beam lengths obtained from LiDAR-RGB and photogrammetric point clouds

	LiDAR-RGB point cloud				Photogrammetric point cloud			
	Measured (m)				Measured (m)			
Span	Average	SD	Design (m)	Measured/design	Average	SD	Design (m)	Measured/design
Left	46.862	0.046	46.837	1.0005	46.710	0.0121	46.837	0.9973
Mid	46.789	0.045	46.837	0.9990	46.707	0.0137	46.837	0.9972
Right	46.791	0.029	46.837	0.9990	46.710	0.0476	46.837	0.9973
Average	46.814	—	—	—	46.709	—	—	—

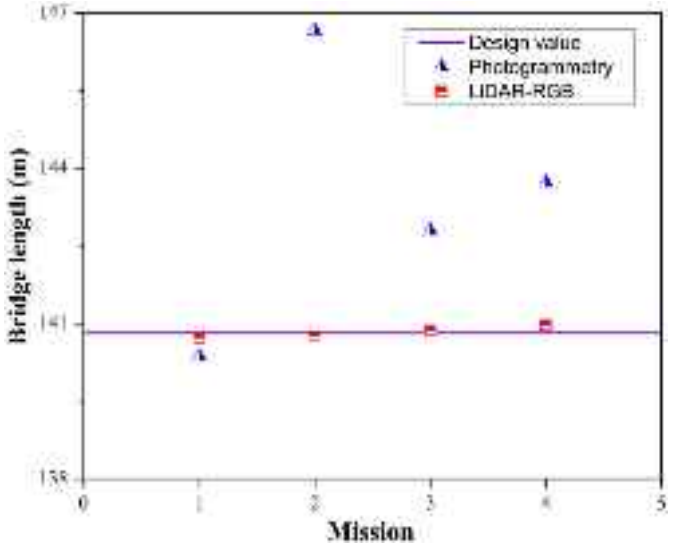

Fig. 15. Bridge length obtained from the LiDAR-RGB and photogrammetric point clouds.

they averaged 146.660 m in the second mission, versus the designed 140.813 m, a discrepancy of approximately 5.8 m.

A similar analysis was employed to measure the out-to-out width of the bridge, which has a design value of 19.5 m. A total of 30 points were selected randomly from the north and south edges of the bridge deck and used to perform linear fitting (Fig. 16) following the steps described previously. For brevity, out-to-out width is reported only for Mission 4. The estimated average bridge width evaluated from the LiDAR-RGB point cloud was 19.50 m, with a standard deviation of 0.031 m, which is in excellent agreement with the design value. The photogrammetric data set yielded a value of 19.58 m and a standard deviation of 0.052 m, which is a slightly greater deviation from the design value, but still satisfactorily accurate.

Discussion

This section provides a detailed description of the most significant factors for achieving satisfactory accuracy in the 3D reconstruction, with reference to specific examples from the presented case study.

Flight Parameters

The quality of the point clouds collected from a UAV-based LiDAR system is highly dependent on the flight conditions, including flight pattern and lateral overlap, flight speed, and altitude. The following conclusions can be drawn from the analyses herein.

1. A parallel flight pattern is suitable for bridge surveying, allowing for reduced flight time and postprocessing requirements in comparison to a transverse flight pattern. In this study, a single grid flight plan with four longitudinal passes was selected, resulting in point clouds with satisfactory density. Fig. 17 illustrates the influence of the number of longitudinal strips on the final quality of the obtained point clouds. Using only one strip may result in the incomplete mapping of portions of the bridge, which might prevent the calculation of the lengths of the spans and/or the entire bridge. Conversely, employing two strips allowed for sufficient information to be collected. Opting for three strips [Fig. 17(d)] resulted in a highly dense point cloud and a detailed description of the construction site. For the case study reported herein, it can be concluded that a single grid flight path, comprising two longitudinal strips, can provide a sufficiently robust data set for comprehensive

Table 3. Bridge lengths obtained from LiDAR/RGB and photogrammetric point clouds

	LiDAR /RGB point cloud				Photogrammetric point cloud			
	Measured (m)				Measured (m)			
Mission	Average	SD	Design (m)	Measured/design	Average	SD	Design (m)	Measured/design
1	140.727	0.077	140.813	0.9994	140.366	0.058	140.813	0.9968
2	140.757	0.042	140.813	0.9996	146.660	0.034	140.813	1.0415
3	140.864	0.056	140.813	1.0004	142.788	0.036	140.813	1.0140
4	140.970	0.077	140.813	1.0011	143.723	0.033	140.813	1.0206
Average of all missions	140.830	—	—	—	143.384	—	—	—
SD	0.111	—	—	—	2.602	—	—	—

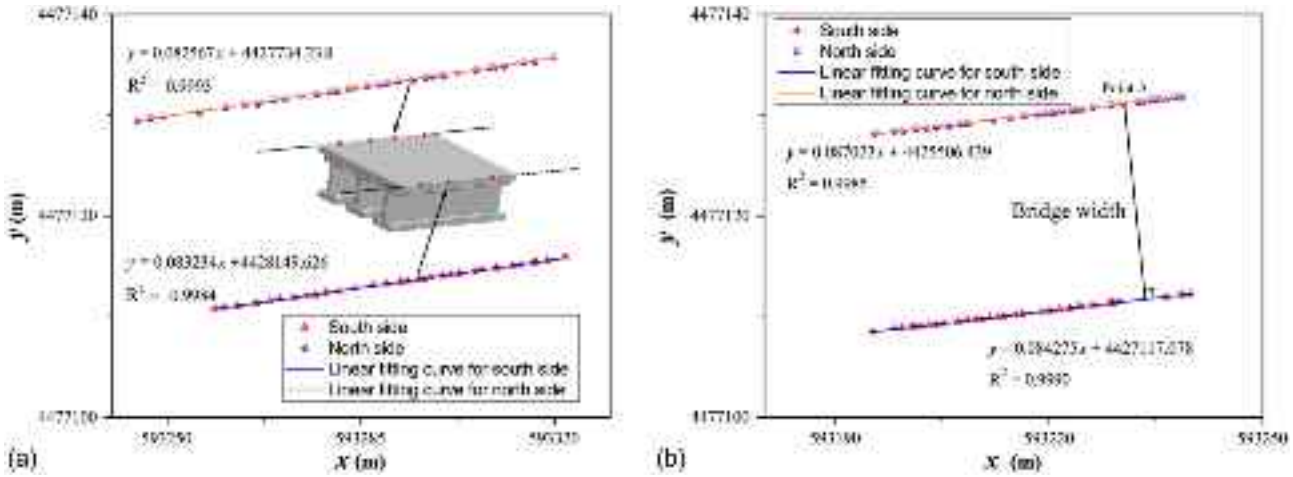

Fig. 16. Evaluation of bridge width based on Mission 4: (a) LiDAR-RGB; and (b) photogrammetry.

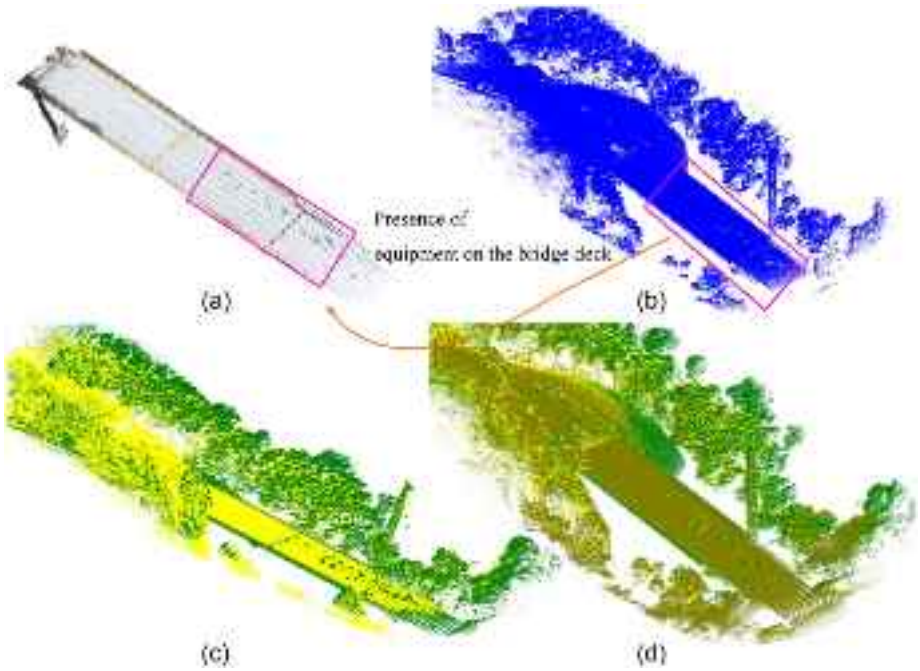

Fig. 17. LiDAR point clouds obtained from different flight strips (Mission 1): (a) LiDAR-RGB data fusion; (b) LiDAR data for Strip 2; (c) LiDAR data for Strips 1 and 2; and (d) LiDAR data for Strips 1, 2, and 3.

bridge scanning while minimizing data collection and postprocessing requirements.
2. The flight path should be planned carefully to cover the entire structure. Due to the presence of residential areas on the east side of the bridge, the flight path planned in this study was designed asymmetrically. As a result, the 3D reconstructions had significant differences in point density; the west side of the bridge had values as much as two times greater than the east end (Fig. 10).
3. The influence of the longitudinal flight speed on the obtained point cloud is significant. A lower flight speed of 8.05 km/h resulted in point clouds with as much as ~46% greater density than a higher flight speed of 11.26 km/h.
4. Flight elevation plays an important role in the final quality of both the LiDAR and RGB data sets. Due to the complexity of the construction site and surrounding environment, the flight altitude often is constrained by the presence of construction machinery, and careful planning and accurate sensor selection are required to obtain the desired reconstruction quality. The potential need to adjust flight elevation between missions brings challenges in resulting variable point cloud densities and noise levels.

Weather Conditions

The operational principle of LiDAR sensors, which measure distances by illuminating a target with laser light and measuring the return time, ensures that the generated data points are substantially unaffected by weather and lighting conditions. In contrast, weather conditions can significantly impact the quality of aerial images captured by RGB sensors. Under- or overexposure resulting from varying weather conditions (including midflight changes), and the presence of shadows or inconsistent illumination, may impact the interpretation of details in the imagery and lower the contrast, leading to poor orthomosaic images and potentially less-accurate point clouds with higher noise levels (Fig. 8). To mitigate these impacts, accurate calibration of the sensor parameters needs to be performed prior to each flight, to match the current conditions and ensure consistent quality.

Lessons Learned and Best Practices

Based on the reported case study of the Fern Hollow Bridge reconstruction, lessons learned are summarized and best practices are proposed for the application of UAV-based LiDAR-RGB systems in bridge construction monitoring operations.

1. The UAV flight path should be scheduled and constantly revised to align with the main construction stages. To mitigate the impact of environmental conditions on the quality of the collected RGB data, it is recommended to conduct operations on sunny days with good lighting conditions.
2. The flight altitude should be selected carefully based on the optimal scanning range of the available LiDAR sensor and camera optics. The flight speed, as discussed previously, should be selected based on the required point cloud density, operational time (including maximum UAV flight speed), and environmental conditions (i.e., wind speed and direction). Based on the reported results, a flight speed between 8.0 and 11.0 km/h provided point clouds with sufficient density to perform geometrical assessment of structural components.
3. A parallel flight path is recommended for bridge surveying, because it can produce point clouds with satisfactory density and accuracy while significantly reducing total flight time and postprocessing requirements. A sufficient side overlap between adjacent flight strips should be maintained, which can be optimized by the flight altitude and the horizontal fields of view of the LiDAR.
4. The RGB data may require preprocessing using image processing software in order to increase the contrast between the target and the environment before generating photogrammetric point clouds and orthomosaic images. Accurate sensor calibration should be performed on the ground before every mission, with particular attention devoted to calibrating the sensor's light sensitivity.
5. Registration algorithms such as the ICP method and sample consensus initial alignment (SAC-IA) should be employed to perform preliminary alignment of the obtained point clouds. Fine alignment then should be performed to increase the quality of the point clouds and avoid overfitting.
6. Although PPK can significantly enhance the accuracy of the positional data, ensuring the reliability and precision of the data set still requires rigorous quality control measures. Quality control checks such as cross-validation with ground control points or reference data can be employed to assure the reliability of the fused results.

Open Challenges and Future Research

This study examined the effectiveness and reliability of UAV-based LiDAR-RGB data fusion to facilitate bridge construction QA/QC. Although the preliminary experimental research formally verified the accuracy of the obtained point clouds, several technical and scientific challenges remain to be addressed.

1. Accuracy. The reported results show that the accuracy of the LiDAR systems in measuring the slope and grade, width, and length of the bridge was satisfactory, exhibiting deviations from the known design values within ~0.1%. However, different applications might require higher levels of accuracy. For example, detecting changes in vertical displacement in bridge systems over time still is an open challenge within civil engineering research. Hence, an essential focus for further research involves enhancing the accuracy of the captured LiDAR point cloud, in terms of both sensor capabilities and optimization of flight parameters.
2. Postprocessing. Postprocessing of large data sets is a complex set of operations that requires trained users. For example, alignments between point cloud strips and between point clouds and the orthomosaic images require specific expertise and are generally time-consuming. To mitigate this challenge, the development of unsupervised algorithms to automatically and accurately identify corresponding points and/or surfaces in adjacent strips to ensure accurate registration is a promising avenue for further research. In particular, the augmentation of the LiDAR point cloud with RGB data fusion creates the potential to devise novel algorithms to increase the accuracy of the alignments, by virtue of the added color information.
3. Data integration. The as-built information obtained from LiDAR and photogrammetric reconstructions has the potential to be integrated into the construction processes and documentation in order to deliver actionable insights for construction managers, which is critical for on-the-ground decision-making throughout the construction of complex large-scale structural systems.

Conclusions

An experimental investigation was carried out to assess the capability of LiDAR-RGB data fusion to monitor bridge construction in the context of QA/QC, with the ultimate goal of assisting

construction management and providing methodologies to quantitatively evaluate construction quality and compliance. Four-dimensional models of the Fern Hollow Bridge reconstruction were created through data fusion of LiDAR and photogrammetric information. The accuracy of the LiDAR point clouds was investigated by comparing the metrics of the bridge geometry against their respective design values. Furthermore, factors influencing the quality and accuracy of the point clouds were discussed, and the potential use of the collected data and avenues for further research were highlighted. The main conclusion can be summarized as follows:

1. LiDAR-RGB point clouds offer a valuable resource for bridge construction QA/QC. They facilitate quantitative observation and measurement of construction operations, bringing the potential to enable deeper levels of as-built information to be recorded over time.
2. Compared with traditional photogrammetric reconstructions, the LiDAR-RGB point clouds had superior accuracy and spatial density, as well as lower noise levels, resulting in a significant increase in the quality of information obtained from the models, such as dimensions of structural elements and geometrical features of the bridge (i.e., longitudinal grade).
3. The flight speed can significantly impact the density of the point cloud; slower speeds result in denser point clouds. Therefore flight path planning is essential for the comprehensive reconstruction of the area of interest, as well as the safety of mapping operations.
4. The generated LiDAR-RGB data have the potential to serve as digitalized as-built documentation. As demonstrated herein, the geometry of the target structural elements can be measured accurately from the point clouds, which also could provide detailed information on the reinforcement layouts. Moreover, direct quantitative comparison of subsequent construction phases is enabled by georeferencing of the scenes, performed using PPK.
5. The challenges of adopting a UAV-based system to monitor the construction process and assess construction quality involve not only the accuracy of point cloud and RGB information captured by the sensors but also the optimization of flight parameters and environmental factors. In addition, the alignments between point cloud strips and the alignments between point clouds and RGB data require specific expertise and generally are time-consuming, which still poses significant practical challenges. Therefore, further research is needed to develop algorithms that can automatically identify and align point cloud strips and/or RGB data, increasing alignment accuracy and improving post-processing efficiency.
6. This study primarily focused on reconstructing the geometry of bridge structural elements during construction using LiDAR-RGB data fusion. Although detailed small-scale information, such as rebar distribution, can be obtained using the proposed methodology, further research is required to assess the feasibility and accuracy of the measurements. Moreover, UAV-based solutions have the potential to incorporate a diverse array of sensors to obtain postconstruction information on internal elements (e.g., by employing ground penetrating radars).

Data Availability Statement

Some or all data, models, or codes that support the findings of this study are available from the corresponding author upon reasonable request.

Acknowledgments

The material presented herein is based upon work supported by the National Science Foundation under Grant CMMI-2232206. Any opinions, findings, and conclusions or recommendations expressed in this material are those of the authors and do not necessarily reflect the views of the National Science Foundation. The authors acknowledge support from the Pennsylvania Department of Transportation, City of Pittsburgh, and Swank Construction Company for the coordination required for the execution of the data collection operations. The help from Trey Blystone in the alignment of selected data is gratefully acknowledged.

References

ACI (American Concrete Institute). 2010. *Specification for tolerances for concrete construction and materials (ACI 117-10) and commentary (ACI 117R-10)*. Farmington Hills, MI: American Concrete Institute.

An, P., J. Liang, K. Yu, B. Fang, and J. Ma. 2022. "Deep structural information fusion for 3D object detection on LiDAR–camera system." *Comput. Vision Image Understanding* 214 (Jan): 103295. https://doi.org/10.1016/j.cviu.2021.103295.

Ariyachandra, M. R. M. F., and I. Brilakis. 2020. "Detection of railway masts in airborne LiDAR data." *J. Constr. Eng. Manage.* 146 (9): 04020105. https://doi.org/10.1061/(ASCE)CO.1943-7862.0001894.

Bai, Y., J. Huan, and S. Kim. 2012. "Measuring bridge construction efficiency using the wireless real-time video monitoring system." *J. Manage. Eng.* 28 (2): 120–126. https://doi.org/10.1061/(ASCE)ME.1943-5479.0000061.

Battulwar, R., G. Winkelmaier, J. Valencia, M. Z. Naghadehi, B. Peik, B. Abbasi, B. Parvin, and J. Sattarvand. 2020. "A practical methodology for generating high-resolution 3D models of open-pit slopes using UAVs: Flight path planning and optimization." *Remote Sens.* 12 (14): 2283. https://doi.org/10.3390/rs12142283.

Benzon, H.-H., X. Chen, L. Belcher, O. Castro, K. Branner, and J. Smit. 2022. "An operational image-based digital twin for large-scale structures." *Appl. Sci.* 12 (7): 3216. https://doi.org/10.3390/app12073216.

Cha, G., S. Park, and T. Oh. 2019. "A terrestrial LiDAR-based detection of shape deformation for maintenance of bridge structures." *J. Constr. Eng. Manage.* 145 (12): 04019075. https://doi.org/10.1061/(ASCE)CO.1943-7862.0001701.

Cheng, L., Y. Wu, Y. Wang, L. Zhong, Y. Chen, and M. Li. 2015. "Three-dimensional reconstruction of large multilayer interchange bridge using airborne LiDAR data." *IEEE J. Sel. Top. Appl. Earth Obs. Remote Sens.* 8 (2): 691–708. https://doi.org/10.1109/JSTARS.2014.2363463.

Chetverikov, D., D. Svirko, D. Stepanov, and P. Krsek. 2002. "The trimmed iterative closest point algorithm." In Vol. 3 of *Proc., 2002 Int. Conf. on Pattern Recognition*, 545–548. New York: IEEE. https://doi.org/10.1109/ICPR.2002.1047997.

Dorafshan, S., and M. Maguire. 2018. "Bridge inspection: Human performance, unmanned aerial systems and automation." *J. Civ. Struct. Health Monit.* 8 (3): 443–476. https://doi.org/10.1007/s13349-018-0285-4.

Ellenberg, A., A. Kontsos, F. Moon, and I. Bartoli. 2016. "Bridge deck delamination identification from unmanned aerial vehicle infrared imagery." *Autom. Constr.* 72 (Dec): 155–165. https://doi.org/10.1016/j.autcon.2016.08.024.

Fascetti, A., and C. Oskay. 2019. "Multiscale modeling of backward erosion piping in flood protection system infrastructure." *Comput.-Aided Civ. Infrastruct. Eng.* 34 (12): 1071–1086. https://doi.org/10.1111/mice.12489.

Garg, P., F. Moreu, A. Ozdagli, M. R. Taha, and D. Mascareñas. 2019. "Noncontact dynamic displacement measurement of structures using a moving laser Doppler vibrometer." *J. Bridge Eng.* 24 (9): 04019089. https://doi.org/10.1061/(ASCE)BE.1943-5592.0001472.

González-Jorge, H., J. Martínez Sánchez, L. Díaz-Vilariño, I. Puente, and P. Arias. 2016. "Automatic registration of mobile LiDAR data using high-reflectivity traffic signs." *J. Constr. Eng. Manage.* 142 (8): 04016022. https://doi.org/10.1061/(ASCE)CO.1943-7862.0001143.

He, M., Q. Zhu, Z. Du, H. Hu, Y. Ding, and M. Chen. 2016. "A 3D shape descriptor based on contour clusters for damaged roof detection using airborne LiDAR point clouds." *Remote Sens.* 8 (3): 189. https://doi.org/10.3390/rs8030189.

Jiang, Z., X. Shen, M. H. Ibrahimkhil, K. Barati, and J. Linke. 2022. "Scan-vs-BIM for real-time progress monitoring of bridge construction project." *ISPRS Ann. Photogramm. Remote Sens. Spatial Inf. Sci.* 10 (Oct): 97–104. https://doi.org/10.5194/isprs-annals-X-4-W3-2022-97-2022.

Jimenez-Cano, A. E., P. J. Sanchez-Cuevas, P. Grau, A. Ollero, and G. Heredia. 2019. "Contact-based bridge inspection multirotors: Design, modeling, and control considering the ceiling effect." *IEEE Robot Autom. Lett.* 4 (4): 3561–3568. https://doi.org/10.1109/LRA.2019.2928206.

Ju, Y., C. Kim, and H. Kim. 2012. "RFID and CCTV-based material delivery monitoring for cable-stayed bridge construction." *J. Comput. Civ. Eng.* 26 (2): 183–190. https://doi.org/10.1061/(ASCE)CP.1943-5487.0000134.

Karan, E. P., R. Sivakumar, J. Irizarry, and S. Guhathakurta. 2014. "Digital modeling of construction site terrain using remotely sensed data and geographic information systems analyses." *J. Constr. Eng. Manage.* 140 (3): 04013067. https://doi.org/10.1061/(ASCE)CO.1943-7862.0000822.

Luo, H., C. Wang, C. Wen, Z. Cai, Z. Chen, H. Wang, Y. Yu, and J. Li. 2016. "Patch-based semantic labeling of road scene using colorized mobile LiDAR point clouds." *IEEE Trans. Intell. Transp. Syst.* 17 (5): 1286–1297. https://doi.org/10.1109/TITS.2015.2499196.

Mac, V. H., Q. H. Tran, J. Huh, N. S. Doan, C. Kang, and D. Han. 2019. "Detection of delamination with various width-to-depth ratios in concrete bridge deck using passive IRT: Limits and applicability." *Materials* 12 (23): 3996. https://doi.org/10.3390/ma12233996.

Navon, R., and Y. Shpatnitsky. 2005. "Field experiments in automated monitoring of road construction." *J. Constr. Eng. Manage.* 131 (4): 487–493. https://doi.org/10.1061/(ASCE)0733-9364(2005)131:4(487).

NTSB (National Transportation Safety Board). 2023. "Improving the identification, prioritization, and completion of follow-up actions on bridges with uncoated weathering steel components." Accessed May 3, 2023. https://www.ntsb.gov/investigations/AccidentReports/Reports/HIR2307.pdf.

Okamoto O., H. Tsuboi, H. Namie, and A. Yasuda. 1997. "Application of RTK-GPS to immersion of caisson." In *Proc., Int. Association of Geodesy Symposia*, edited by J. Segawa. Heidelberg, Germany: Springer.

Omar, T., and M. L. Nehdi. 2017. "Remote sensing of concrete bridge decks using unmanned aerial vehicle infrared thermography." *Autom. Constr.* 83 (Nov): 360–371. https://doi.org/10.1016/j.autcon.2017.06.024.

Parsamehr, M., U. S. Perera, T. C. Dodanwala, P. Perera, and R. Ruparathna. 2023. "A review of construction management challenges and BIM-based solutions: Perspectives from the schedule, cost, quality, and safety management." *Asian J. Civ. Eng.* 24 (1): 353–389. https://doi.org/10.1007/s42107-022-00501-4.

Pennsylvania DOT. 2022. "Fern Hollow Bridge project." Accessed March 11, 2022. https://www.penndot.pa.gov/RegionalOffices/district-11/ConstructionsProjectsAndRoadwork/AlleghenyCountyConstruction/Pages/FernHollowBridgeProject.aspx.

Puri, N., and Y. Turkan. 2020. "Bridge construction progress monitoring using lidar and 4D design models." *Autom. Constr.* 109 (Jan): 102961. https://doi.org/10.1016/j.autcon.2019.102961.

Qureshi, A. H., W. S. Alaloul, A. Murtiyoso, S. J. Hussain, S. Saad, and M. A. Musarat. 2024. "Smart rebar progress monitoring using 3D point cloud model." *Expert Syst. Appl.* 249 (Sep): 123562. https://doi.org/10.1016/j.eswa.2024.123562.

Resop, J. P., L. Lehmann, and W. C. Hession. 2019. "Drone laser scanning for modeling riverscape topography and vegetation: Comparison with traditional aerial lidar." *Drones* 3 (2): 35. https://doi.org/10.3390/drones3020035.

Rusu, R. B., Z.-C. Márton, N. Blodow, M. E. Dolha, and M. Beetz. 2008. "Towards 3D point cloud based object maps for household environments." *Robotics Autom. Syst.* 56 (11): 927–941. https://doi.org/10.1016/j.robot.2008.08.005.

Schnabel, R., R. Wahl, and R. Klein. 2007. "Efficient RANSAC for point-cloud shape detection." *Comput. Graph. Forum* 26 (2): 214–226. https://doi.org/10.1111/j.1467-8659.2007.01016.x.

Seo, J., L. Duque, and J. Wacker. 2018. "Drone-enabled bridge inspection methodology and application." *Autom. Constr.* 94 (Oct): 112–126. https://doi.org/10.1016/j.autcon.2018.06.006.

Shirowzhan, S., S. M. E. Sepasgozar, and J. Trinder. 2021. "Developing metrics for quantifying buildings' 3D compactness and visualizing point cloud data on a web-based app and dashboard." *J. Constr. Eng. Manage.* 147 (3): 04020178. https://doi.org/10.1061/(ASCE)CO.1943-7862.0001971.

Sohn, G., and I. Dowman. 2007. "Data fusion of high-resolution satellite imagery and LiDAR data for automatic building extraction." *ISPRS J. Photogramm. Remote Sens.* 62 (1): 43–63. https://doi.org/10.1016/j.isprsjprs.2007.01.001.

Spencer, B. F., Jr., V. Hoskere, and Y. Narazaki. 2019. "Advances in computer vision-based civil infrastructure inspection and monitoring." *Engineering* 5 (2): 199–222. https://doi.org/10.1016/j.eng.2018.11.030.

Trepekli, K., T. Balstrøm, T. Friborg, B. Fog, A. N. Allotey, R. Y. Kofie, and L. Møller-Jensen. 2022. "UAV-borne, LiDAR-based elevation modelling: A method for improving local-scale urban flood risk assessment." *Nat. Hazards* 113 (1): 423–451. https://doi.org/10.1007/s11069-022-05308-9.

Trzeciak, M., and I. Brilakis. 2023. "Dense 3D reconstruction of building scenes by AI-based camera–lidar fusion and odometry." *J. Comput. Civ. Eng.* 37 (4): 04023010. https://doi.org/10.1061/JCCEE5.CPENG-4909.

Uddin, W. 2008. "Airborne laser terrain mapping for expediting highway projects: Evaluation of accuracy and cost." *J. Constr. Eng. Manage.* 134 (6): 411–420. https://doi.org/10.1061/(ASCE)0733-9364(2008)134:6(411).

Wallace, L., A. Lucieer, C. Watson, and D. Turner. 2012. "Development of a UAV-LiDAR system with application to forest inventory." *Remote Sens.* 4 (6): 1519–1543. https://doi.org/10.3390/rs4061519.

Wang, M., and X. Yin. 2022. "Construction and maintenance of urban underground infrastructure with digital technologies." *Autom. Constr.* 141 (Sep): 104464. https://doi.org/10.1016/j.autcon.2022.104464.

Wang, Q., J. C. P. Cheng, and H. Sohn. 2017. "Automated estimation of reinforced precast concrete rebar positions using colored laser scan data." *Comput.-Aided Civ. Infrastruct. Eng.* 32 (9): 787–802. https://doi.org/10.1111/mice.12293.

Xu, Z., Y. Liang, Y. Xu, Z. Fang, and U. Stilla. 2022. "Geometric modeling and surface-quality inspection of prefabricated concrete components using sliced point clouds." *J. Constr. Eng. Manage.* 148 (9): 04022087. https://doi.org/10.1061/(ASCE)CO.1943-7862.0002345.

Yan, Y., Z. Mao, J. Wu, T. Padir, and J. F. Hajjar. 2021. "Towards automated detection and quantification of concrete cracks using integrated images and lidar data from unmanned aerial vehicles." *Struct. Control Health Monit.* 28 (8): e2757. https://doi.org/10.1002/stc.2757.

You, H., F. Xu, and J. Du. 2023. "Improved boundary identification of stacked objects with sparse LiDAR augmentation scanning." *J. Constr. Eng. Manage.* 149 (11): 04023104. https://doi.org/10.1061/JCEMD4.COENG-13626.

Yuan, X., A. Smith, F. Moreu, R. Sarlo, C. D. Lippitt, M. Hojati, S. Alampalli, and S. Zhang. 2023. "Automatic evaluation of rebar spacing and quality using LiDAR data: Field application for bridge structural assessment." *Autom. Constr.* 146 (Feb): 104708. https://doi.org/10.1016/j.autcon.2022.104708.

Yuan, X., A. Smith, R. Sarlo, C. D. Lippitt, and F. Moreu. 2021. "Automatic evaluation of rebar spacing using LiDAR data." *Autom. Constr.* 131 (Nov): 103890. https://doi.org/10.1016/j.autcon.2021.103890.

Zhang, S., C. Liu, K. Feng, C. Xia, Y. Wang, and Q. Wang. 2024. "Computer vision-based real-time monitoring for swivel construction of bridges: From laboratory study to a pilot application." *Eng. Constr. Archit. Manage.* https://doi.org/10.1108/ECAM-10-2022-0992.

Zhong, X., X. Peng, S. Yan, M. Shen, and Y. Zhai. 2018. "Assessment of the feasibility of detecting concrete cracks in images acquired by unmanned aerial vehicles." *Autom. Constr.* 89 (May): 49–57. https://doi.org/10.1016/j.autcon.2018.01.005.